Geoscience and Remote Sensing (2024)
Clausius Scientific Press, Canada

DOI: 10.23977/geors.2024.070103
ISSN 2523-2592 Vol. 7 Num. 1

An Alternative Fast Seismic Site Classification Method Based on Geological Maps: A Case Study in Shandong Province, North China

Zhiheng Li[1,2], Hongtai Xu[1,*], Chengyu Liu[1], Hongwei Wang[1], Yulong Zhang[1]

[1]*Shandong Earthquake Agency, Ji'nan, 250014, China*
[2]*Institute of Geophysics, China Earthquake Administration, Beijing, 100081, China*
[*]*Corresponding author*

Keywords: Geologic age, Quaternary Sediment type, Borehole data, Site classification

Abstract: We propose an alternative fast seismic site classification method here based on geological maps. Geological maps contain a large amount of geological information, such as rock hardness, geologic age, and Quaternary sediment genesis, which may build links for seismic site classification. In this paper, a workflow for rapid seismic site categorization was established by taking Shandong Province in China as an example. Based on the database constructed by extracting relevant information from geological maps, this paper presents the specific rules for seismic site classification. Firstly, rock hardness was considered as a first-level criterion for the direct classification of Class I and Class II sites. Then, for sites that cannot be directly classified by rock hardness, the geological age and Quaternary sedimentary genesis are used as the second level of criteria to classify the sites. Further, the collected borehole data verifies the accuracy of the seismic site classification results. Our method provides a new perspective for rapid seismic site categorization, and in particular, can be used in an area where no actual drilling has taken place.

1. Introduction

The intensity of surface movement is highly dependent on seismic site (referred to as site hereafter) characteristics [1]. The site serves as the medium through which seismic waves propagate, and the essence of seismic disasters lies in the response of sites to intense seismic motion. Site conditions primarily include geological factors such as topography, geological structures, soil type, and properties, as well as the thickness of the soil deposit [2-4]. Different sites exhibit varying responses under the earthquake, especially for soft soil layers where seismic waves tend to undergo significant amplification, resulting in incredible destruction [5-8].

Researchers conducting seismic damage investigations near the epicenter of the 1906 San Francisco earthquake observed significant differences in building damage across different site categories [9]. Likewise, during the 1985 Mexico earthquake, despite occurring along the Pacific coast, the seismic destruction was concentrated in Mexico City, approximately 400 km away from the epicenter, due to the site amplification effect of the Mexico Basin’s lacustrine deposits [10]. Subsequent earthquakes, such as the Tangshan earthquake, Chi-Chi earthquake, and Wenchuan

earthquake, further confirmed the influence of different site types on seismic motion [11-13]. Consequently, the classification of sites based on different geological conditions has become an important research direction in the field of seismic geology and plays a crucial role in regional seismic hazard prediction and rapid assessment.

The indicator approach is widely used internationally to categorize sites, but the indicators vary by country[14-16]. The United States, Europe, etc. use the average shear wave velocity (V_{S30}) within the top 30 meters of the subsurface soil and rock layers as the basis for site classification [17-18]. The Chinese Code for Seismic Design of Buildings GB50011-2010 primarily relies on two indicators for site classification [19], i.e., the thickness of the overlying soil layer and the equivalent shear wave velocity within the top 20 meters of the soil layer. However, whether using a single indicator like in the United States or dual indicators in China, on-site geological surveys are still necessary to obtain shear wave velocity data from soil and rock layers, which require significant engineering effort and economic investment [20-23]. Since obtaining borehole velocity data can often be challenging, in recent years, many researchers have used readily available geological and topographical data to establish correspondences between traditional indicator-based site classification and various geological parameters. Park and Elrick classified the Quaternary, Paleogene, and Neogene/Cretaceous formations in California, USA based on different shear wave velocities. They divided them into three types of sites based on geological ages, providing corresponding V_{S30} values. They established a relationship model between the NEHRP site categories and geological factors, using V_{S30} as a bridge, and completed the site classification in California [24]. Wills et al. collected V_{S30} data from over 1,200 boreholes and 1:250,000-scale geological maps in California, and statistically analyzed the corresponding relationships between geological units and V_{S30} values, resulting in the classification of seven types of sites based on shear wave velocity [25]. Wills et al. further used large-scale geological maps to refine the geological unit and site category relationship matrix by validating drilling and near strong-motion stations' geological boundaries and determining their shear wave velocity characteristics [26]. Subsequently, Lee et al. conducted a simple geological classification of Taiwan based on different scales of geological data, sedimentary ages, and lithology. They completed the site classification for free-field seismic stations in Taiwan and validated the results using strong motion records and response spectrum shape (RSS) and horizontal-to-vertical spectral ratio (HVSR) methods [27]. D. Shi et al. established a relationship matrix between geological units and NEHRP site categories based on geological origins and ages and used the correspondence between Chinese and American specifications to obtain a site classification map according to Chinese standards [28]. These researchers developed site classification methods based on geological data. However, previous studies focused on exploring the relationship between site classification and single factors extracted from geological data, which were limited and not systematic. In addition, the accuracy of these classification methods has not been verified by actual measurement data, nor have they been applied in a particular region.

This paper presents an alternative methodology and a workflow for rapid seismic site classification. We first extracted some geological parameters (geological age, rock hardness, and Quaternary sediment genesis) from the geological map of Shandong Province, China, and constructed a site classification database. Then, based on the correlation law between geological factors and the site classification indexes, we established a multi-parameter classification method and drew the site classification map of Shandong Province. Finally, the accuracy of the site classification results is verified by the collected borehole data.

2. Geological Overview and Drilling Data of the Shandong Province

Shandong Province is located on the eastern coast of China, on the lower reaches of the Yellow River. The landforms within its territory are complex and varied, ranging from alluvial plains to hilly mountains. Overall, the terrain is featured by center high and surrounding low. Jiaodong Peninsula located in the eastern of Shandong Province is a hilly area, dominated by a low mountainous landscape with wide valleys slow slopes, and gentle undulations, while the central part of Shandong Province is high and hilly, belonging to the central-southern hilly area. The landforms of the north-west and south-west are characterized by the plains formed by the alluvial deposits of the Yellow River, that is, the north-west and south-west plains of Shandong Province, which are part of the North China Plain [29-30]. Stratigraphy from the Archean to Cenozoic is distributed in the area, and strata of other ages are exposed, except for the lack of Lower Ordovician, Silurian, Devonian, and Lower Carboniferous age strata, of which the Cenozoic strata are most exposed, followed by Paleozoic strata. The distribution of Proterozoic strata is limited, and Paleozoic strata are sporadically exposed. The Quaternary deposits are dominated by fluvial, fluvial-bed, and marine sedimentary complexes, accompanied by swampy, flooded, wind-accumulated, and lacustrine deposits [31-33].

We collected a total of 1192 well-distributed engineering geological boreholes in the study area, which contain lithological profiles and shear wave velocity data. In particular, shear wave velocity data were obtained by surface excitation and in-well excitation method with a sampling point step of 1m in the soil layer [34]. The lithological profile data show that fine-grained sediments such as silt and silty clay are more common in boreholes, reflecting a relatively low-energy sedimentary environment. The columnar diagram of the soil profile of a typical borehole and the corresponding shear-wave velocity profile of this borehole are shown in Figure 1.

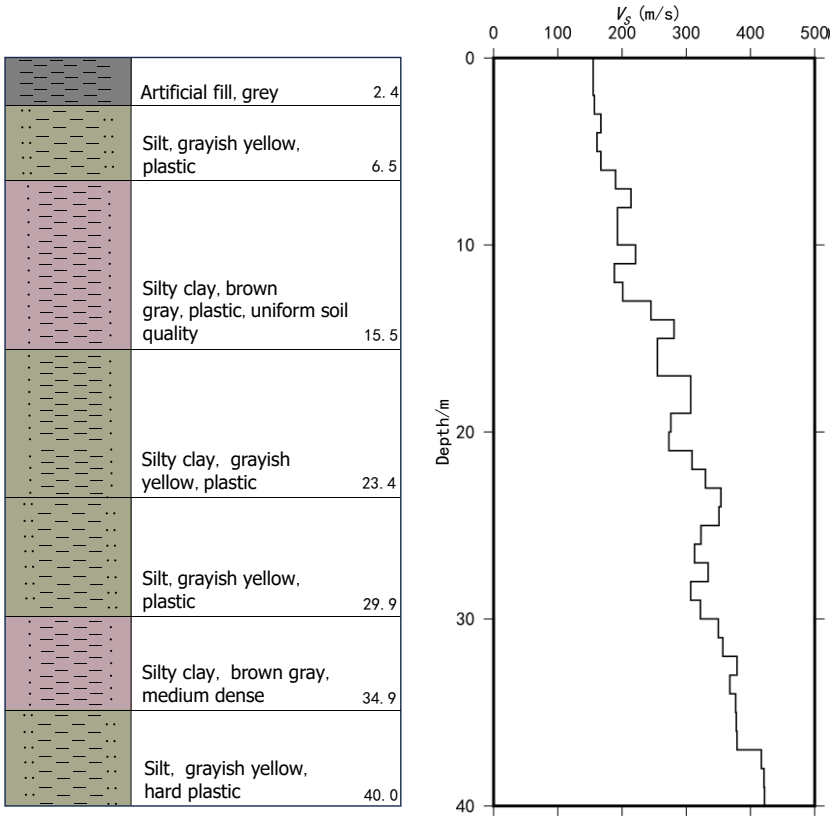

Figure 1: Lithological histograms and corresponding shear wave velocity profiles of typical drill holes in the Shandong Province

3. Geological database construction

By collecting a 1:500,000 scale geological map (referred to as geological map hereafter) and compiling 1,192 engineering borehole data, we constructed a site classification database based on geological factors.

3.1. Statistics on Quaternary sediment types

Quaternary strata are widely developed in Shandong Province, and most of the soils in the current project site are Quaternary sediments, mainly deposited on land or in basins, including particles of silt, clay, sand, and gravel. According to the types of Quaternary sediment genesis, we extracted information from geological maps and classified them into eight categories: river alluvial deposits, marine deposits, sea-land interaction deposits, lacustrine deposits, marsh accumulations, slope deposits, aeolian deposits, and river alluvial-pluvial deposits. The specific distribution is shown in Figure 2.

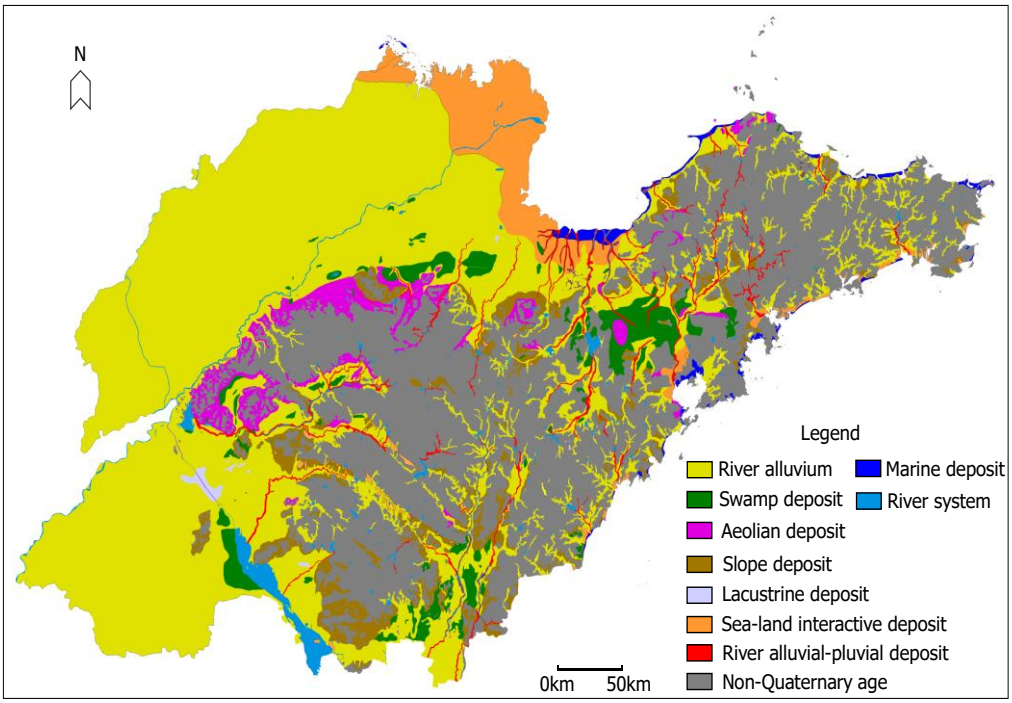

Figure 2: Distribution map of Quaternary sediment Genesis in Shandong Province

3.2. Statistics of rock hardness

According to China's Standard for engineering classification of rock mass (GB50218-2014) [35], rock bodies can be qualitatively classified into five types based on their hardness (Table 1). We extracted information on the lithology and lithology combination from the geological map, classifying the rock hardness grades into four basic categories according to Table 1 as follows:

a. Hard rock, mainly including granite, gabbro, basalt, diorite, andesite, rhyolite, peridotite, marble, quartzite, etc.

b. Sub-hard rock, mainly including tuff, diorite, dolomite, chert, gneiss, dioritic hornblende, quartz schist, and so on.

c. Soft rock, mainly including mudstone, sandstone, conglomerate, clay rock, shale, gypsum rock, marl, feldspar sandstone, coarse conglomerate, and so on.

Table 1: Qualitative classification table of rock hardness classes

Name	Representative rock
Hard rock	Unweathered - slightly weathered granite, anorthosite, diorite, diorite, gabbro, basalt, andesite, gneiss, quartzite, quartz sandstone, etc.
Sub-hard rock	Unweathered - slightly weathered marble, slate, dolomite, limestone, etc.
Sub-soft rock	Moderately weathered hard and sub-hard rocks; unweathered - slightly weathered tuffs, sandy mudstones, marl, siltstones, sandstones, sandy shales, etc.
Soft rock	Strongly weathered hard and sub-hard rocks; moderately weathered softer rocks; unweathered - slightly weathered muddy sandstones and mudstones, etc.
Extremely soft rock	Fully weathered rocks of all kinds; strongly weathered soft rocks; and various semi-diagenetic rocks.

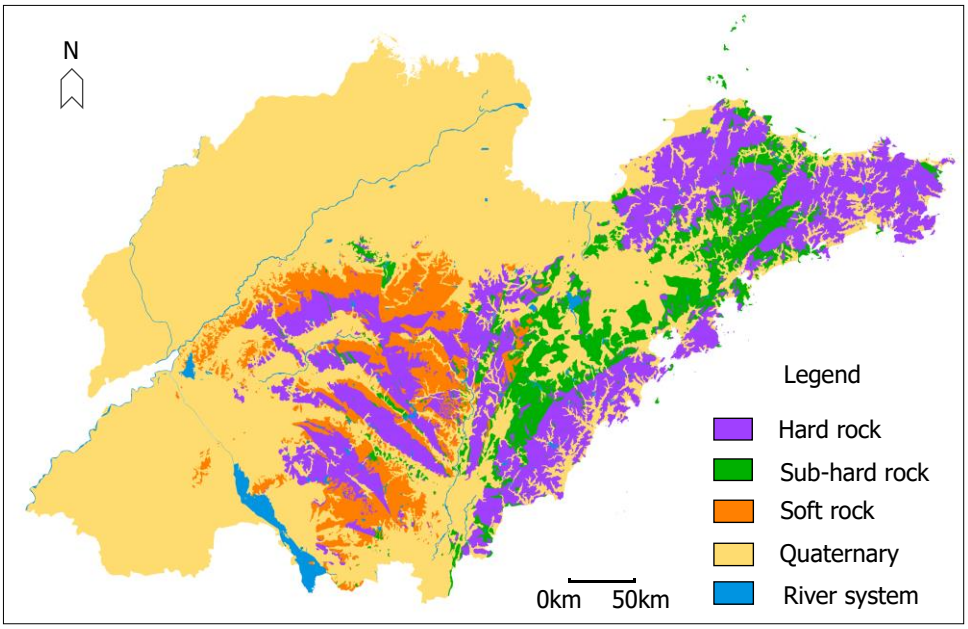

Figure 3: Distribution of rock hardness in Shandong Province

From the distribution map of rock hardness (Fig. 3), hard rocks, sub-hard rocks, and soft rocks are distributed over a large area in the hilly areas of south-central Shandong. The eastern hills are dominated by hard rocks, interspersed with some sub-hard rocks, accompanied by a sporadic distribution of soft rocks. In general, there is a wide distribution of hard rocks, and the rocks from the plains to the mountains are characterized by an increasing number of hard rocks.

3.3. Borehole data

The data of drill holes we used here, including their locations, lithology data, and 30-m average shear wave speed (V_{S30}). We have analyzed the geological information of each borehole and classified it based on the geological age. The results indicate that 814 boreholes are situated in the Quaternary Holocene strata (Qh), 122 boreholes are located in the Quaternary Pleistocene strata (Qp), 6 boreholes are situated in the Neogene strata (N), 9 boreholes are located in the Paleogene strata (E), 127 boreholes are positioned in the Mesozoic strata (Mz), and 114 boreholes are located in the Paleozoic and older strata (Pz^{+}). Considering that the Holocene is the newest stratigraphy in Quaternary, we further subdivided it into the upper (Qh_1), middle (Qh_2), and lower (Qh_3)

Quaternary Holocene according to lithologic descriptions, with 411, 378, and 25 drill holes, respectively.

The Box diagram (Figure 4) shows the distribution of V_{S30} corresponding to the geologic ages involved based on the drill hole data, in which, the center marker, the box edges, and the whiskers represent the median (50th percentile), the 25th and 75th percentiles, and 1.5 times the interquartile spacing, respectively. It's worth noting that a few data outside the whiskers are likely to be outliers and should be eliminated. As seen in Figure 5, the data of median V_{S30} shows a clear upward trend from newer to older geologic ages indicating that the strata become harder as the age of deposition increases. As a consequence, the shear wave velocities also increase accordingly.

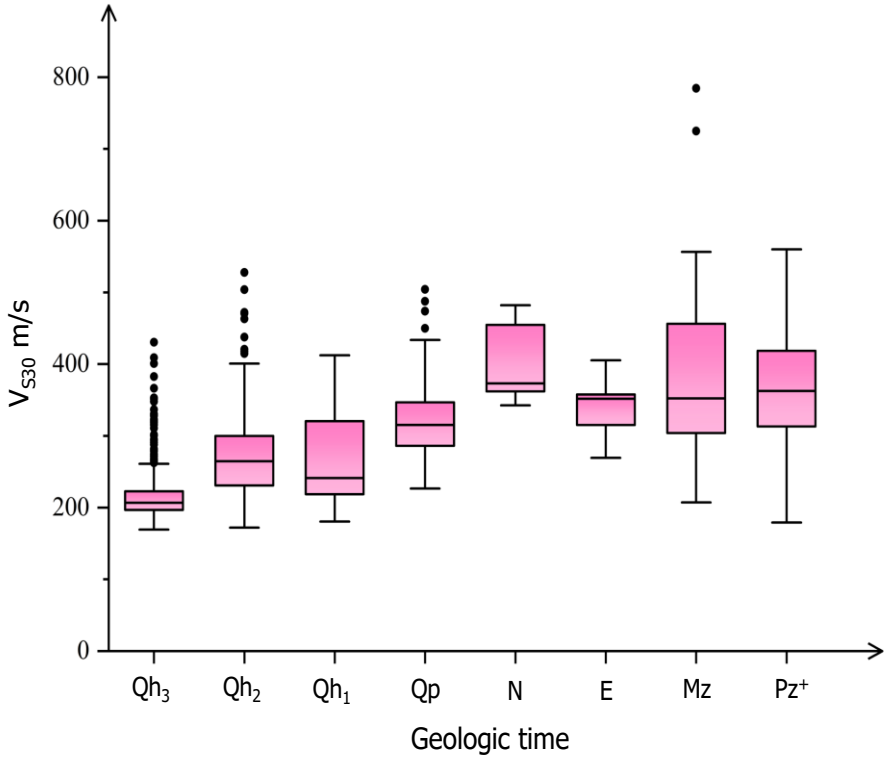

Figure 4: Distribution of V_{S30} corresponding to different geological ages

In addition, we came across some irregularities, in particular the unusual decline in the median V_{S30} in the lower Holocene of the Quaternary and the uncommon increase in the median V_{S30} in the Neoproterozoic. We believe that the inadequate borehole data available for these geological periods may be a plausible explanation for these anomalies.

4. Methods of site classification based on geological factors

Two indicators including the thickness of the soil layer and the equivalent shear wave velocity of the soil layer within 20 meters depth are used to determine the site classification in China. Noteworthily, if shear wave velocity test data is not available, soil types are used as an alternative to classification. Soil types are routinely divided into four categories, i.e., hard or rocky soil, medium-hard soil, medium-soft soil, and soft soil (See Table 2). A general principle is the harder the soil, the more likely it is to be classified as a Class I or II site. The sites of stable rock and dense gravelly soil are directly classified as Class I regardless of the thickness of the overburden. Whereas the medium-hard soil with an overburden thickness of more than 5 meters is classified as a Class II site. The above information can be used as an empirical basis for classifying sites based on geological

factors.

Table 2: Definitions of site classes in the Chinese seismic code GB50011-2010

Type of soil	Geotechnical names and properties	Equivalent shear wave velocity V_{Se}	Thickness of soil layer, H (m)				
			I_0	I_1	II	III	IV
Hard soil or rock	Stable rock, dense gravelly soil	$V_S>800$	0				
		$800\geq V_S>500$		0			
Sub-hard soil	Moderately dense, slightly dense gravelly soils, dense, moderately dense gravel, coarse to medium sand $f_{ak}\leq 200$ Clayey and chalky soils, hard loess	$500\geq V_{Se}>250$		<5	≥5		
Sub-soft soil	Slightly dense gravels, coarse and medium sands, fine and chalky sands except loose, clayey, and chalky soils with $f_{ak}\leq 130$, fills with $f_{ak}>130$, plastic loess.	$250\geq V_{Se}>140$		<3	3~50	>50	
Soft soil	Silt and silty soils, loose sands, recently deposited clayey and chalky soils, $f_{ak}\leq 130$ fills, plastic loess.	$V_{Se}\leq 140$		<3	3~15	>15~80	>80

Referring to Table 2, we classified the site of hard and sub-hard rocks as Class I and soft rocks as Class II based on rock hardness. However, the site classification of Quaternary is difficult to define directly based on rock hardness. Therefore we can further classify the site categories concerning Quaternary sediment genesis.

River alluvial deposits are formed through long-term surface water flow transportation in the impact plain, river terrace, and delta zone accumulation, generally deposited in the upper reaches of the river for coarse-grained material, the middle reaches of the deposited material for medium-coarse-grained material, downstream of the deposited material for the clay and other fine-grained material, with a clear laminar structure [36]. Flood deposits are materials formed by temporary flooding from large amounts of rainfall or large amounts of snowmelt over a short period, which washes debris from the hillside and accumulates it at the exit of a ravine or on the slower plains in front of a hill [36]. Marine sediments are deposits formed by the action of waves, tides, and currents, as well as by the action of marine organisms [36]. Aeolian deposits are sedimentary materials in arid regions formed by the dynamic action of winds, blowing up from areas of strong winds and landing and accumulating in areas of weak winds. Based on the general understanding that the older the geologic age, the harder the lithology and the higher the shear wave velocity, we classify Holocene alluvial, flood, marine, and aeolian deposits as Class III sites, and Pleistocene alluvial, flood, marine, and wind deposits are classified as Class II sites.

Lacustrine deposits and marsh accumulations are usually distributed in shallow water along the lakeshore, dominated by coarser-grained sand and gravel deposits of relatively small thickness. Whereas, in deeper water at the center of the lake dominated by fine-grained chalk and clay

deposits, the thickness of which can generally reach tens of meters or even hundreds of meters. Thus, the Holocene lacustrine and marsh deposits are classified as Class IV sites, and the lacustrine and marsh deposits of other Quaternary geologic ages are classified as Class III sites. In addition to the above types of sediments, the remaining portion of relatively hard sediments are uniformly classified as Class II sites.

In the attribute table of the geological map, we divided the rock hardness into 3 groups and the Quaternary sediments into 8 groups according to their genesis, selecting geological age, classification of rock and soil bodies, and type of sediments as geological parameters. Further, we adopt the principle of multi-parameter grading classification to classify the sites.

a. We take the degree of rock hardness as the first level and directly classify some of the sites of Class I and Class II.

b. For the sites that can't be directly classified by the degree of rock hardness, we use the Quaternary sediment genesis in conjunction with the geological age as the second level for classifying the sites.

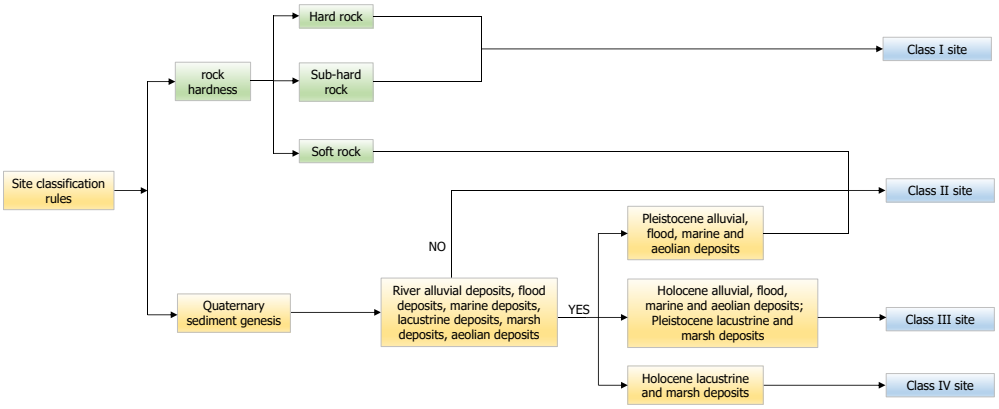

Figure 5: Flowchart of site classification rules based on geologic factors

The flow of site classification rules based on geological factors is shown in Figure 5. Adopting the methods we proposed above, a fast site classification map for Shandong Province based on geological factors was drawn (Figure 6).

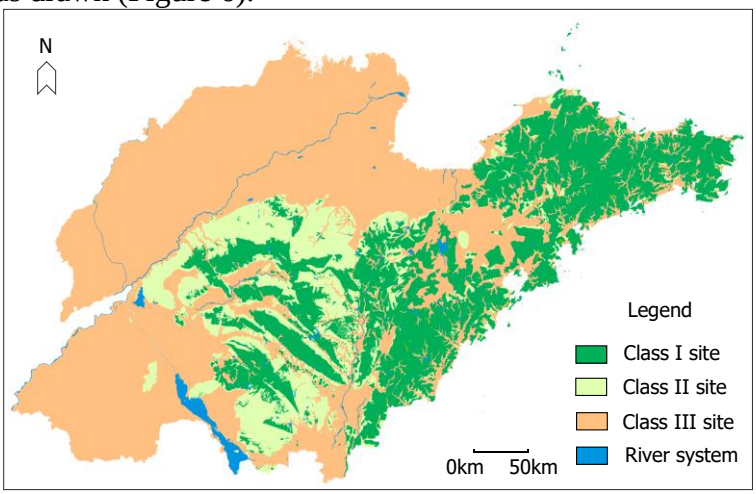

Figure 6: Classification map of sites in Shandong Province based on geological factors

As seen in Figure 6, the distribution of the different classes of sites can be well observed. Class III sites are primarily located in the plain areas of the northwest and southwest of the study area. Class I sites are dominant in the hilly areas in the eastern part, whereas Class II sites are more

prevalent in the hilly areas in the south-central part. However, in the southeast of the south-central hilly areas of Shandong Province, Class I sites are more common. The Holocene lacustrine and marsh accumulations are classified as Class IV sites, however, these categories are very rare. In addition, the large scale of the geologic map data collected for this study, further leads to the fact that the areas to which Class IV sites belong are not well displayed in the Site Classification Map. Thus, we show only Class I, II, and III sites in the Site Classification Map, which fully meets the research needs.

5. Comparative validation of measured borehole data

We used 1192 measured borehole data to validate the reasonableness of the site classification method we proposed above. In Figure 7, we plot the site classification results which are measured by boreholes together with the Site Classification Map. It can be seen that the results of class I, class II, and class III site classification are generally consistent with most of the measured borehole points. Undeniable, there are some deviations between the measured borehole data and classification scheme, which may be attributed to the larger scale of the geological map we used, resulting in some geological units not being well distinguished.

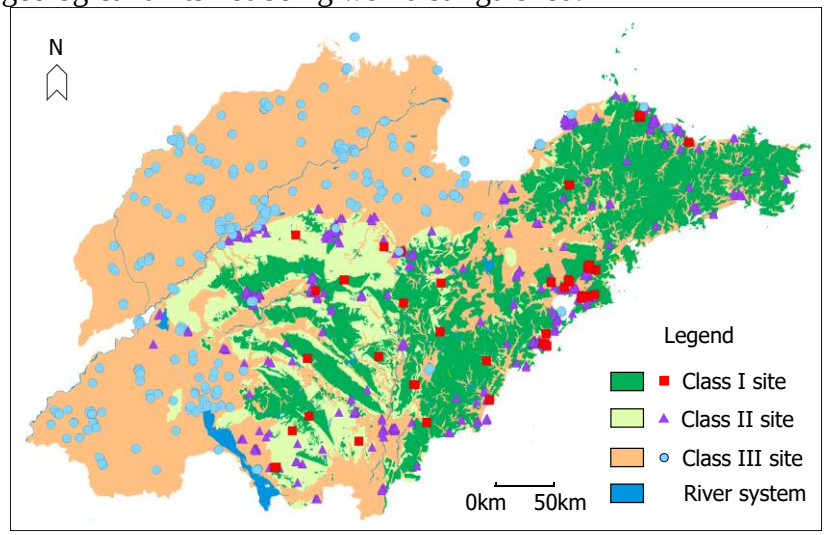

Figure 7: Comparison chart for validation of measured borehole data

We further analyzed the statistics according to different site types. The study shows that 241 measured drill holes were distributed within the area of the Class I site, of which 176 belonged to the Class I site, with an accuracy rate of 73%. Considering the Class II site area, a total of 167 drill holes were extracted, of which 142 of the measured drill holes belong to Class II sites, reaching a high accuracy rate of 85%. Meanwhile, a total of 814 drill holes were extracted within the Class III site area, of which 642 belonged to Class III sites, with an accuracy of 78%. The validation results show high confidence, demonstrating that the method of site classification by geological factors we proposed is feasible.

6. Conclusion

In this paper, we present an alternative methodology to establish seismic site classification. We use the geological map of Shandong Province, China, to extract geological parameters and construct a site classification database based on geological factors. Then, based on the correlation law between geological factors and the site classification indexes in China, we proposed a multi-parameter classification method. Finally, the reasonableness of the site classification method we

proposed above is validated by measured borehole data. The main conclusions are drawn as follows:

1) We constructed a database containing information on geological maps, in which Quaternary sediments are classified into eight categories and rock hardness grades are classified into three categories.

2) By analyzing the correspondence between the rock hardness grading in the geological map and the soil type classification, the relationship between geologic factors and site classification indexes was established based on Chinese site classification standards, as well as a site classification scheme based on geologic factors.

3) The measured data of boreholes validate the reliability of the site categorization method we proposed, which can serve as a reference for the classification of sites in areas without actual boreholes.

4) Although our method has proved to be highly reliable, it can only be relied upon for rough categorization, and the precise definition of site categories based on geological factors proposed in this paper remains limited.

Acknowledgements

We thank two anonymous reviewers for their constructive and helpful comments to improve this manuscript. This work was jointly supported by the scientific research project of Shandong Earthquake Agency (YB2407) and Key Task of Earthquake Emergency and Information Technology for Distinguished Young Scholars of China Earthquake Administration (CEAITNS202321)

References

[1] Montessus, D. Seismic history of southern Los Andes south of parallel 16". Santiago, Chile: Cervantes Barcelona press; 1911. (In Spanish).

[2] Di Capua, G.; Peppoloni, S.; Amanti, M.; Cipolloni, C.; Conte, G. Site classification map of Italy based on surface geology. Geological Society, London, Engineering Geology Special Publications 2016, 27, 147-158.

[3] Forte, G.; Chioccarelli, E.; De Falco, M.; Cito, P.; Santo, A.; Iervolino, I. Seismic soil classification of Italy based on surface geology and shear-wave velocity measurements. Soil Dynamics and Earthquake Engineering 2019, 122, 79-93.

[4] Crespo, M.; Benjumea, B.; Moratalla, J.; Lacoma, L.; Macau, A.; González, Á.; ... Stafford, P. A proxy-based model for estimating V_{S30} in the Iberian Peninsula. Soil Dynamics and Earthquake Engineering 2022, 155, 107165.

[5] Ren, Y.; Zhou, Y.; Wang, H.; Wen, R. Source characteristics, Site effects, and path attenuation from spectral analysis of strong-motion recordings in the 2016 Kaikōura earthquake sequence. Bulletin of the Seismological Society of America 2018, 108, 1757-1773.

[6] Ji, K.; Wen, R.; Ren, Y.; Dhakal, Y. Nonlinear seismic site response classification using K-means clustering algorithm: A case study of the September 6, 2018, Mw6.6 Hokkaido Iburi-Tobu earthquake, Japan. Soil Dynamics and Earthquake Engineering 2020, 128, 105907.

[7] Fu, L.; Xie, J.; Chen, S.; Zhang, B.; Zhang, X.; Li, X. Analysis of site amplification coefficient characteristics of Sichuan and its application in strong ground-motion simulation: A case study of 2022 Lushan M_S6.1 earthquake. Chinese Journal of Geophysics 2023, 66, 2933-2950.

[8] Liu, Y.; Zhao, X.; Wen, Z.; Liu, J.; Chen, B.; Bu, C.; Xu, C. Broadband ground motion simulation using a hybrid approach of the May 21, 2021 M7. 4 earthquake in Maduo, Qinghai, China. Earthquake Science 2023, 36, 175-199.

[9] Hansen, R.; Hansen, G. 1906 San Francisco earthquake. South Carolina: Arcadia Publishing 2013.

[10] Ramos-Martínez, J.; Chávez-García, F.; Romero-Jiménez, E.; Rodríguez-Zúñiga, J.; Gómez-González, J. Site effects in Mexico City: constraints from surface wave inversion of shallow refraction data. Journal of Applied Geophysics 1997, 36,157—165.

[11] Wen, Z.; Xie, J.; Gao, M.; Hu, Y.; Chau, K. Near-source strong ground motion characteristics of the 2008 Wenchuan earthquake. Bulletin of the Seismological Society of America 2010, 100, 2425-2439.

[12] Xie, J. Strong-Motion Directionality and Evidence of Rupture Directivity Effects during the Chi-Chi M w 7.6 Earthquake. Bulletin of the Seismological Society of America 2019, 109, 2367-2383.

[13] An, Z.; Xie, J.; Zhang, Y.; Li, X. J.; Wen, Z. Rupture directivity effect on strong ground motion during the 12 May

2008 M_W7. 9 Wenchuan earthquake. Earthquake Science 2021, 34, 234-245.
[14] Zhou, J.; Li, X.; Tian, X.; Xu, G. New Framework of Combining Observations with Topographic Slope to Estimate VS30 and Its Application on Building a V_{S30} Map for China. Bulletin of the Seismological Society of America 2022, 112, 2049-2069.
[15] Xie, J.; Li, K.; Li, X.; An, Z.; Wang, P. V_{S30}-based relationship for Chinese site classification. Engineering Geology 2023, 324, 107253.
[16] Liu, W.; Juang, C.; Peng, Y.; Chen, G. Regional characterization of V_{S30} with hybrid geotechnical and geological data. Underground Space 2023, 11, 218-231.
[17] Building Seismic Safety Council. NEHRP Recommended Seismic Provisions for New Buildings and Other Structures. Building Seismic Safety Council, Federal Emergency Management Agency 2020, Washington D.C.
[18] European Committee for Standardization. EUROCODE 8: Design of structures for earthquake resistance Part 1: General rules, seismic actions, and rules for buildings 2014. London.
[19] Ministry of Housing and Urban-rural Development of the People's Republic of China, General Administration of Quality Supervision, Inspection and Quarantine of the People's Republic of China. GB50011-2010 Code for Seismic Design of Buildings. Beijing: China Architecture & Building Press 2016, 18-20.
[20] Xie, J.; Zimmaro, P.; Li, X.; Wen, Z.; Song, Y. V_{S30} Empirical Prediction Relationships Based on a New Soil-Profile Database for the Beijing Plain Area, China. Bulletin of the Seismological Society of America 2016, 106, 2843–2854. https://doi.org/10.1785/0120160053.
[21] Xie, J.; Li, X.; Wen, Z.; Jia, L.; An, Z.; Cui, J.; Lin, G.; Zhang, Q.; Jiang, P.; Xie, Q.; Wang, P.; Zimmaro, P.; Stewart, J.P. Soil Profile Database and Site Classification for National Strong-Motion Stations in Western China. Seismological Research Letters 2022, 93, 1930–1942. https://doi.org/10.1785/0220210271.
[22] Jia, L.; Xie, J.; Li, X.; Wen, Z.; Chen, W.; Zhou, J. Empirical prediction models of time-averaged shear wave velocity V_{S20} and V_{S30} in Sichuan and Yunnan areas. Acta Seismologica Sinica 2021, 43, 628-642+679. (in Chinese with English abstract).
[23] Ji, K.; Ren, Y.; Wen, R.; Zhu, C.; Liu, Y.; Zhou, B. HVSR-based Site Classification Approach Using General Regression Neural Network (GRNN): Case Study for China Strong Motion Stations. Journal of Earthquake Engineering 2022, 26, 8423–8445. https://doi.org/10.1080/13632469.2021.1991520
[24] Park, S.; Elrick, S. Predictions of shear-wave velocities in Southern California using surface geology. Bulletin of the Seismological Society of America 1998, 88, 677-685.
[25] Wills, C.; Petersen, M.; Bryant, W.; Reichle, M.; Saucedo, G.; Tan, S.; Taylor, G.; Treiman, J. A Site-Conditions Map for California Based on Geology and Shear-Wave Velocity. Bulletin of the Seismological Society of America 2000, 90, S187-S208.
[26] Wills, C.; Clahan, K. Developing a map of geologically defined site-condition categories for California. Bulletin Seism Soc Am 2006, 96,1483-1501.
[27] Lee, C.; Cheng, C.; Liao, C.; Tsai, Y. Site classification of Taiwan free-field strong-motion stations. Bulletin of the Seismological Society of America 2001, 91, 1283-1297.
[28] Shi, D.; Wen, R.; Ren, Y.; Zhou, B. The Study of Site Classification Based On GIS. Geomatics World 2011, 9,23-27. (in Chinese with English abstract).
[29] Song, M. The Composing, Setting and Evolution of Tectonic Units in Shandong Province. Geological Survey and Research 2008, 3, 165-175. (in Chinese with English abstract).
[30] Liu, C.; Li, G.; & Liu, F. Early Cretaceous-Cenozoic exhumation history of Luxi Terrane and adjacent areas, eastern North China Craton. Geological Journal 2022, 57, 2735-2748.
[31] Wang, Z.; Jia, R.; Sun, Z.; Shi, R.; Chao, H. Geometry and activity of the Anqiu-Zhuli segment of the Anqiu-Juxian Fault in the Yishu fault zone, Seismology and Geology 2005, 27, 212-220. (in Chinese with English abstract).
[32] Wang, Z.; Wang, D.; Xu, H.; Ge, F.; Yang C.; Li J. Geometric features and latest activities of the north segment of the Anqiu-Juxian Fault. Seismology and Geology 2015, 37,176-191. (in Chinese with English abstract).
[33] Wang, H.; Feng, Z.; Liu, X.; Chen, S. Quantitative analysis of site effect on seismic ground motion peak acceleration in the Shandong area. Seismology and Geology 2015, 37, 44-52. (in Chinese with English abstract).
[34] Ge, F.; Wang, D.; Xu, H.; Shen, D.; Liu, X.; Chen, T.; Zhang, Z. Study on the conversion of equivalent shear wave velocity and 30 m equivalent shear wave velocity in Shandong Province. Science Technology and Engineering 2020, 20, 9751-9756. (in Chinese with English abstract).
[35] Ministry of Housing and Urban-rural Development of the People's Republic of China, General Administration of Quality Supervision, Inspection and Quarantine of the People's Republic of China. GB50218 – 2014 Standard for engineering classification of rock mass. Beijing: China Planning Press 2014,4-5.
[36] Shu L. Physical Geology. Beijing: Geological Publishing House 2010.